scientific reports

OPEN

Synthesis of a novel ternary ZIF-8/GO/MgFe₂O₄ nanocomposite and its application in drug delivery

Saleheh Sanaei-Rad[1], Mohammad Ali Ghasemzadeh[1✉] & Seyyed Mohammad Hossein Razavian[2]

In recent year, metal–organic frameworks (MOFs) have been displayed to be a category of promising drug delivery systems because of their crystalline structure, the potential of further functionality, and high porosity. In this research, graphene oxide was synthesized from pure graphite via hummer method and then MgFe₂O₄ nanoparticles was incorporated into the synthesized ZIF-8 metal–organic frameworks which followed with loading on the surfaces of graphene oxide. In continue, tetracycline as an antibiotic drug was loaded on the surfaces and the cavities of the prepared nanocomposite. The outcomes of this research revealed that 90% of the tetracycline was loaded on the synthesized ZIF-8/GO/MgFe₂O₄ nanostructure. Next, drug release was done at pH: 5 and pH: 7.4 within 3 days, resulting about 88% and 92% release of the tetracycline, respectively. With using different spectroscopic methods like X-ray crystallography (XRD), scanning electron microscope (SEM), energy-dispersive X-ray spectroscopy (EDX/Mapping), Fourier transform infrared (FTIR), thermalgravimetric analysis (TGA), and Brunauer–Emmett–Teller (BET), the structure of synthesized materials was confirmed. Furthermore, the antibiotic activity of tetracycline trapped into the ZIF-8/GO/MgFe₂O₄ was evaluated by agar-well diffusion method on both gram-positive (*Staphylococcus aureus*) and gram-negative (*Escherichia coli*) bacteria, which showed good antibacterial results.

In last decade, more attention has been paid to improvement novel techniques for the advancing of drug delivery systems. The increasing numbers of drug resistances in bacterial contaminants have become important healthcare challenges due to the severe reduction in the number of therapy and repetitive treatment accessible. This issue has led to enhanced morbidity developed medicinal. As a result, combination treatment involving the co-application of existing antibiotics with unique nano structures such as metal halides, nano-sized transporters, and metal oxide nanoparticles is a promising approach to counter antimicrobial opposition[1].

The tetracycline (TC) is a type of antibiotics that constrain protein combination by stopping the addition of aminoacyl-tRNA to the ribosomal acceptor (A) sites (Fig. 1)[2].

TCs are broad-spectrum agents, displaying activity against a varied kind of bacteria[3]. The favorable anti-microbial and antifungal attributes of these agents and the loss of mighty adverse side effects has led to their applications in the treatment of animal and human infections. The main feature of this drug is its use at certain hours in order to completely control the infection[2].

Nano-scale carbon allotrope have been extensively investigated by researchers for targeted drug delivery. In this regard, graphene sheets with highly active surfaces are astonishingly desirable for fundamental research and technological applications. This two-dimensional structure has been considered due to having several functional groups connected to carbon plates with high density, biocompatibility, high electrical, and conductivity properties[4].

Graphene oxide (GO) as a kind of graphite derivatives give easy dispensability in water and other organic solvents. GO possess wealthy oxygen containing functionalities such as epoxide, carboxyl, ketone, lactone, and hydroxyl groups[5]. Furthermore, it has a great specific surface area and displays excellent activities which are a versatile tool in chemical transformations[6], and also in drug delivery systems[7].

Metal–organic frameworks have lately concerned very attention in the meantime. MOFs display many basic specifications in drug delivery due to flexible building, variable sizes and figures, easily functionalization, high porosity, easy biodegradability and high design capability[8–10]. ZIF-8 is a type of zeolitic imidazole frameworks (ZIFs) which have excellent benefits because of highly pore sizes, massive surface area and simple variation of

[1]Department of Chemistry, Qom Branch, Islamic Azad University, Qom, Islamic Republic of Iran. [2]Department of Microbiology, Qom Branch, Islamic Azad University, Qom, Islamic Republic of Iran. ✉email: Ghasemzadeh@qom-iau.ac.ir
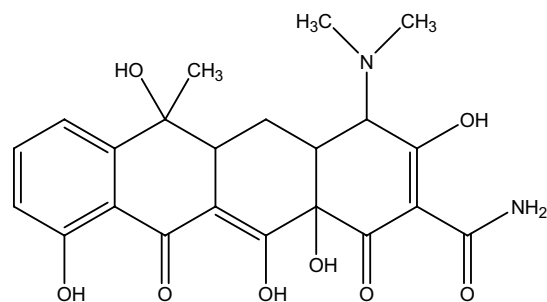
Figure 1. Chemical structure of tetracycline.
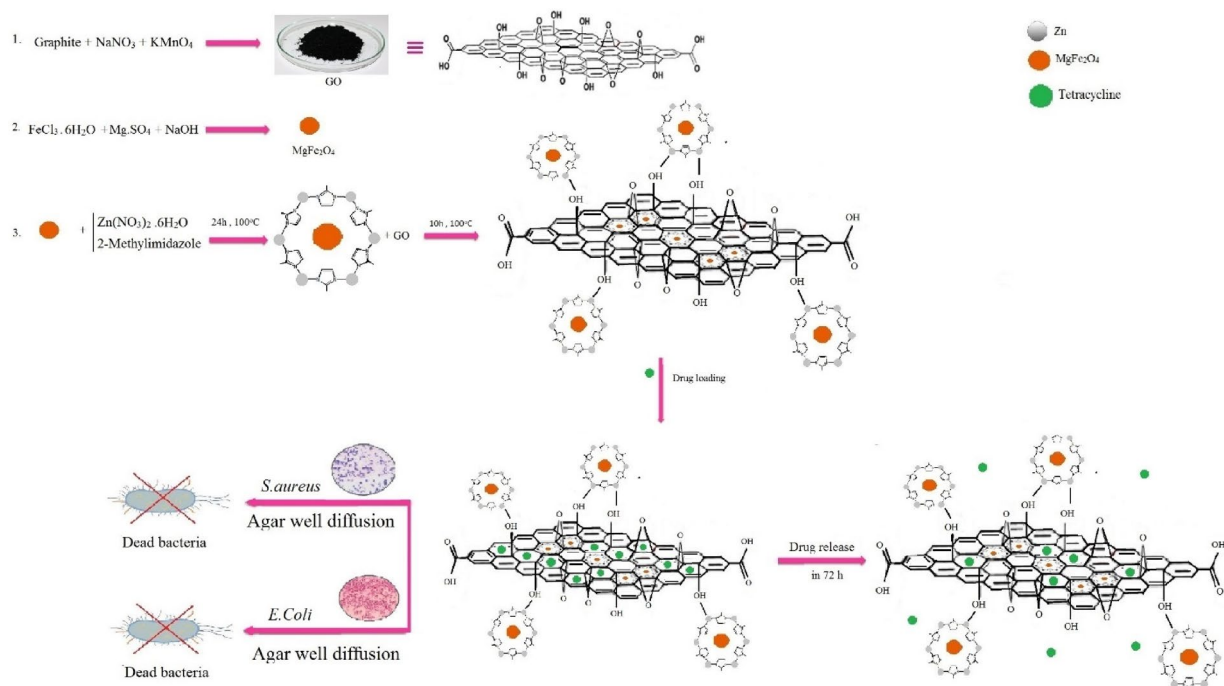
Figure 2. Simulation of the preparation of the ZIF-8/GO/MgFe$_2$O$_4$ framework, drug loading, release and antibacterial tests.

the pore sizes inside the frameworks with modifiable organic groups[11]. However, to improve the stability of the carrier, scientists have been used some metals with high oxidation state (Ni^{2+}, Al^{3+}, Zr^{4+}, Fe^{3+}, Mg^{2+}) to form powerful coordination bond in ligands to provide extremely stable MOFs. Therefore, great oxidation state metal-based MOFs or their composites display considerable potential in antibiotic sensing[12,13].

We used MgFe$_2$O$_4$ nanoparticles with crystal structure in which the particles are rather disordered than crystalline particles, there by having many more defects can provide better nanocarrier concentration and extra active sites. Also, magnetic nanoparticle MgFe$_2$O$_4$ exhibited greater super paramagnetic propriety and homogeneous diameter. This information indicates that Mg (II) is safe and practical to use in a drug delivery systems[14].

Previously, metal–organic framework skeletons have been used as potential nanocarriers in drug delivery of some antibiotics[1,15], folic acid[16], anticancer drugs[17,18] and ibuprofen[19].

Considering the significance of the previous issues associated to discovery of new drug delivery systems to find a suitable and practical nanocarrier[20–22], we were capable to introduce a unique and impressive nanostructure like ZIF-8/GO/MgFe$_2$O$_4$ as a carrier for the loading and release of TC.

Furthermore, the antibacterial activities of the prepared composites were compared and evaluated with pure tetracycline against *Staphylococcus aureus* and *Escherichia coli* bacteria by agar-well diffusion method which exhibited considerable results. The target of the this work was to progress the performance of the antibacterial drug delivery method, and drug release control (Fig. 2).

Experimental

Materials and instruments.   Chemicals materials were bought from the Sigma-Aldrich and Merck in high purity. FT-IR spectra were recorded on Magna-IR spectrometer 550. Powder X-ray diffraction (XRD) was carried out on a Philips diffractometer of X'pert Company with mono chromatized Cu kα radiation (λ = 1.5406 Å). The compositional analysis was done by energy dispersive analysis of X-ray (EDX, Kevex (Newark, DE) Delta Class I). Microscopic morphology of products was visualized by SEM (LEO1455VP). Thermogravimetric analysis (TGA) was performed on a Mettler Toledo TGA under argon and heated from room temperature to 825. The approximate sample weight was 10 mg in TG experiment with 10 °C/min heating rate. Nitrogen adsorption–desorption isotherms were measured at 196 using a Belsorp mini automatic adsorption instrument after degassing the samples at 150 °C for 5 h. Absorption spectra were recorded in the range 200–800 nm on a Shimadzu model.
1601 PC UV–visible spectrophotometer (Shimadzu, Tokyo, Japan).

Synthesis MgFe$_2$O$_4$ nanoparticles.   A mixture of MgSO$_4$ (1.2 g) and FeCl$_3$.6H$_2$O (2.4 g) were dissolved in deionized water (30 mL) was stirred until to afford a clear mixture (Solution A). Then, 3.2 g of NaOH was solved in 15 mL of deionized water by a magnetic stirrer, this solution was labeled as mixture B. Then, the solution B was gradually added to the solution A, which followed under vigorous stirring. Eventually, the solution was transferred in stainless steel pressure vessel. The autoclave was kept at 180 °C for 10 h and then cooled down slowly. The obtained residue was collected, washed three steps with deionized water, dried and then calcinated in a furnace at 700 °C for 3 h[23].

Preparation of ZIF-8/MgFe$_2$O$_4$.   In a backer, MgFe$_2$O$_4$ NPs (0.5 g) and Zn(NO$_3$)$_2$.6H$_2$O (0.6 g) were mixed in methanol (10 mL). In another vessel, 2-methyl imidazole (1.3 g) was poured in methanol (10 mL) and then the mixture was stirred vigorously. Then, two vessels were mixed together and the solution was mixed completely for 30 min. The obtained residue was separated by centrifugation method and was washed several times with methanol. Eventually, the product was dried at 100 °C for 24 h[24].

Synthesis of graphene oxide.   GO was prepared by Hummer's method. Normally, pure graphite (5 g) and sodium nitrate (2.5 g) was added to sulfuric acid (115 mL, 98%) and the solution was equipped to a magnetic stirrer with a condenser which placed in an ice bath. During the stirring of the mixture, KMnO$_4$ (15 g) was added slowly for 120 min.

The mixture was placed in a water bath (35 °C) and stirred for half hour. Next, 230 mL of ultrapure water was gradually added into the mixture and stirring was continued at 98 °C for 15 min. In continue, 700 mL of DI water and H$_2$O$_2$ (50 mL, 30%) were respectively added to the solution to end the reaction. When the reaction completed, the product was washed with HCl (5%) and DI water for three times. The obtained GO was dried at 60 °C for 12 h[25].

Preparation of ZIF-8/GO/MgFe$_2$O$_4$.   A mixture of 0.1 g of ZIF-8/MgFe$_2$O$_4$ nanocomposite and GO (0.5 g) was dispersed in DMF (30 mL) under ultrasonic irradiations and then the mixture was conducted into an autoclave at 100 °C for 10 h. When the reaction was ended, the obtained residue was separated and washed three several times with dimethyl formamide, DI water and ethanol, respectively. Lastly, the prepared ZI F-8/GO/MgFe$_2$O$_4$ was dried at 40 °C for overnight.

Encapsulation of tetracycline into the ZIF-8/GO/MgFe$_2$O$_4$.   In order to drug loading on ZIF-8/GO/MgFe$_2$O$_4$, 0.05 g of the activated ZIF-8/GO/MgFe$_2$O$_4$ powder was mixed with tetracycline (0.1 g) and ultrapure water (5 mL). The suspension solution of ZIF-8/GO/MgFe2O4/TC was stirred for the duration of 5 days at room temperature. Then, the product including tetracycline encapsulated on nanocomposite was separated by centrifuge and washed two times with H$_2$O and EtOH. Finally, the sediment was dried at 40 °C for 24 h. The amount of encapsulated drug was 90% based on   the Eq. (1).

$$\text{Drug loading (\%)} = \big(\text{TC weight in example/total weight of example}\big) \times 100\% \tag{1}$$

Drug release from ZIF-8/GO/MgFe$_2$O$_4$/TC.   The release of tetracycline was investigated in buffer acetate and phosphate buffer saline. In this method, ZIF-8/GO/MgFe$_2$O$_4$/TC (0.02 g) was added to the 50 mL of every buffer, individually. Next, the mixture was stirred at 37 °C for 72 h. Every time, 5 mL of the mixture was removed and replaced with the equal value of the fresh buffer. The value of tetracycline release from the ZIF-8/GO/MgFe$_2$O$_4$/TC composite was checked by UV–Vis spectrometer at 360 nm. It was demonstrated that the drug release according to Eq. (2) was achieved 92% and 88% at pH: 5, and pH: 7.4, respectively.

$$\text{Release percentage (\%)} = \text{mr (amount of released TC)/ml (total amount of loaded TC)}. \tag{2}$$

Antibacterial studies.   The antimicrobial activity of the pure TC, ZIF-8/GO/MgFe$_2$O$_4$, and ZIF-8/GO/MgFe$_2$O$_4$/TC were measured via the agar-well diffusion technique, that fresh cultures of *Escherichia coli* (*E. coli*), and *Staphylococcus aureus* (*S. aureus*), bacteria were used. Initially, Moller agar (40 mL) was incubated into every sterilized Petri plate with the analogous strains of bacteria. The plates were left to solidify at room temperature for 1 day. Afterward, a well of 6 mm diameter was done by a sterile cork borer. Next, 50 and 100 µl of tetracycline,
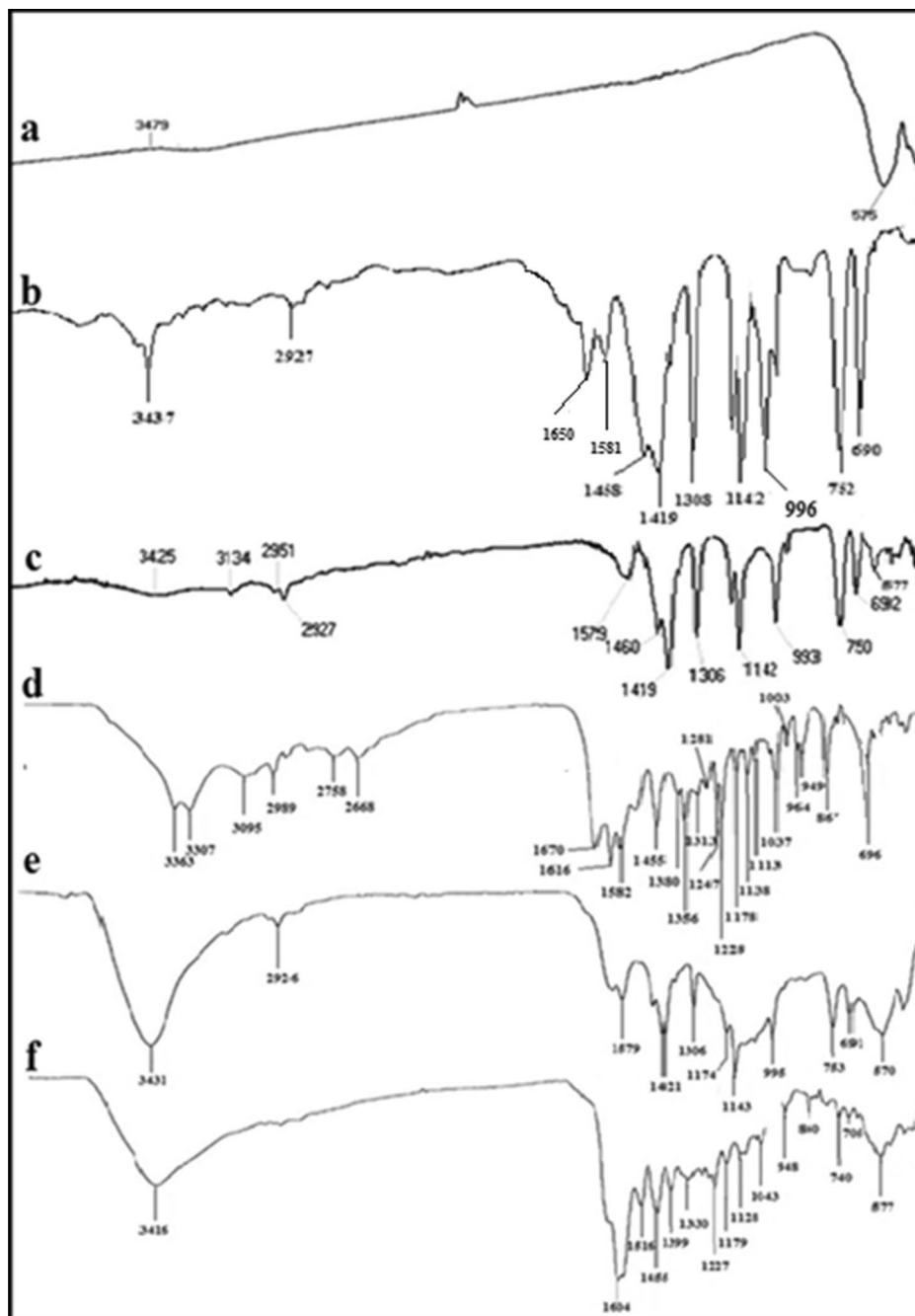
Figure 3. FT-IR spectra of MgFe$_2$O$_4$ (**a**), ZIF-8 (**b**), ZIF-8/MgFe$_2$O$_4$ (**c**), TC (**d**), ZIF-8/GO/MgFe$_2$O$_4$ (**e**), ZIF-8/GO/MgFe$_2$O$_4$/TC (**f**).

ZIF-8/GO/MgFe$_2$O$_4$, and ZIF-8/GO/MgFe$_2$O$_4$/TC which was prepared at a concentration of 10 mg/mL of HCl was transferred in diameter well. Finally, the plates were incubated for overnight at 37 °C.

Results and discussion
FT-IR spectroscopy.   The FT-IR spectra of MgFe$_2$O$_4$, ZIF-8/MgFe$_2$O$_4$, tetracycline, ZIF-8/GO/MgFe$_2$O$_4$, and ZIF-8/GO/MgFe$_2$O$_4$/TC are shown in Fig. 3. The absorption bonds related to Mg–O and Fe–O in MgFe$_2$O$_4$ nanoparticles are appeared at 435 cm^{-1}, and 575 cm^{-1}, respectively (Fig. 3a)[23].

FT-IR spectrum of ZIF-8 is shown in Fig. 3b. As indicated the corresponding absorption bands at 485, 1180, 1581, 1650, and 2927 cm^{-1} are corresponding to Zn–N, C–N, C=C, C=N and C–H, respectively. Figure 3c displays FT-IR spectrum of ZIF-8/MgFe$_2$O$_4$ composite. As illustrated, the stretching vibrations due to Mg–O and Fe–O in MgFe$_2$O$_4$ NPs are appeared at 435 and 575 cm^{-1}. Moreover, the main absorption bonds in ZIF-8
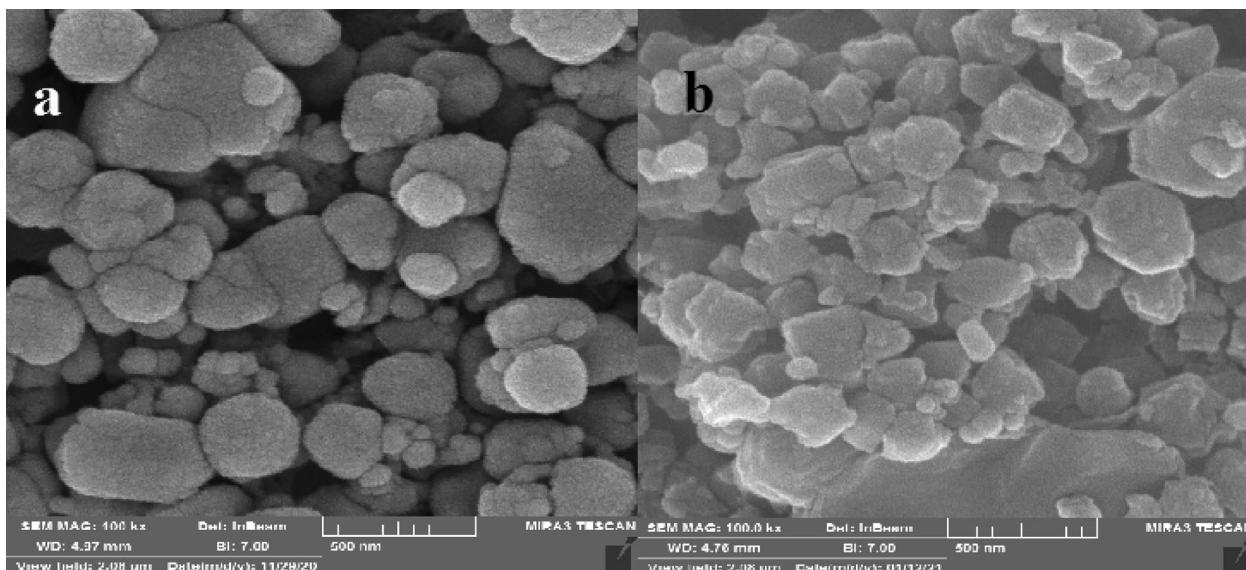
Figure 4. SEM images of ZIF-8/GO/MgFe$_2$O$_4$ **(a)**, and ZIF-8/GO/MgFe$_2$O$_4$/TC **(b)**.

structure are appeared at 2925, 1589 and 485 cm^{-1} due to stretching vibrations of C–H, C=N and Zn–N bonds, respectively[26].

FT-IR spectrum of the pure tetracycline is indicated in Fig. 3d. As indicated, the corresponding peaks because of the presence of OH and NH$_2$ groups were observed at 3363 and 3305 cm^{-1}. Also, The peaks showed the C–H stretching vibrations of aromatic rings from 3095 to 2989 cm^{-1}, C=C stretching from 1582 to 1616 cm^{-1}, and C–N stretching at 1228 cm^{-1}, C=O stretching at 1670 cm^{-1}, and C–O stretching from 1037 to 1113 cm^{-1} [27]. The FT-IR spectrum of ZIF-8/GO/MgFe$_2$O$_4$ displays a broad and intense peak at 3367 cm^{-1} due to stretching vibration of O–H groups in grapheme oxide. The absorption bonds at 1724 cm^{-1} is related to the stretching vibration of carbonyl group at the edges of GO. Whereas, the peaks at 1045 cm^{-1} and 1215 are due to the stretching vibrations of C-O bands (Fig. 3e)[23].

Figure 3f displays the FT-IR spectrum of ZIF-8/GO/MgFe$_2$O$_4$/TC which approves the existence of each component in the structure. The stretching vibrations of Mg–O and Fe–O in MgFe$_2$O$_4$ NPs are shown at 435 and 575 cm^{-1}. The peak at 3367 cm^{-1} is related to the OH groups. The absorption band at 3305 cm^{-1} depends to NH$_2$ moiety of TC, representing the successfully encapsulation of TC into the structure. The absorption bonds at 1724 cm^{-1}, 1045 cm^{-1}, and 1215 cm^{-1} is related to the stretching vibration of carbonyl group, and C–O bonds in the structure of GO.

Field-emission scanning electron microscope analysis. The particle size and morphology of the ZIF-8/GO/MgFe$_2$O$_4$ before and after TC loading are indicated in Fig. 4. SEM illustration of the ZIF-8/GO/MgFe$_2$O$_4$ shows that nanoparticles have almost spherical structure (Fig. 4a). In Fig. 4b, with loading of the TC on the surfaces of the ZIF-8/GO/MgFe$_2$O$_4$ nanocomposite, the particle size was increased and also the morphology of the nanocomposite disordered due to drug loading.

Energy-dispersive X-ray spectroscopy. EDX technique was applied to explore the elemental components of the prepared ZIF-8/GO/MgFe$_2$O$_4$/TC nanocomposite. Figure 5 shows that the elements are including Mg, O, Fe, C, N, and Zn for the ZIF-8/GO/MgFe$_2$O$_4$/TC nanostructure.

Furthermore, EDX analysis has been performed in the mode of elemental mapping of the ZIF-8/GO/MgFe$_2$O$_4$/TC nanocomposite (Fig. 6). The highly dispersive of elements distribution verified that there is no impurity in the prepared nanocomposite. It was found that in the item of C (Fig. 6a), Fe (Fig. 6b), N (Fig. 6c), O (Fig. 6d), Zn (Fig. 6e), and Mg (Fig. 6f) which not only exhibited the excellent purity but also disclosed the homogeneous scattering of elements within the ZIF-8/GO/MgFe$_2$O$_4$/TC. Eventually, Fig. 6g shows the homogeneous arrangement of the elements throughout the structure. Also, SEM imaging in Fig. 6h (10 nm) revealed a few micrometer-sized precipitates, which could not be seen in the SEM images (Fig. 4) due to lower sampling depth.

Brunauer–Emmett–Teller techniques. The BET absorption technique is a suitable method to calculate the surface area and porosity of the structures. As shown in the BET plots (Fig. 7), the available surface areas were 504.56 m^{2}g^{-1} (Fig. 7a) and 131.06 m^2 g^{-1} (Fig. 7b) before and after loading TC, respectively. The pore capacity of the cavities in the ZIF-8/GO/MgFe$_2$O$_4$ is 0.3378 cm^3 g^{-1} which has been decreased to 0.059053 cm^3 g^{-1} after encapsulation of the TC. This information confirm that the encapsulation of the TC in the cages of ZIF-8/GO/MgFe$_2$O$_4$.
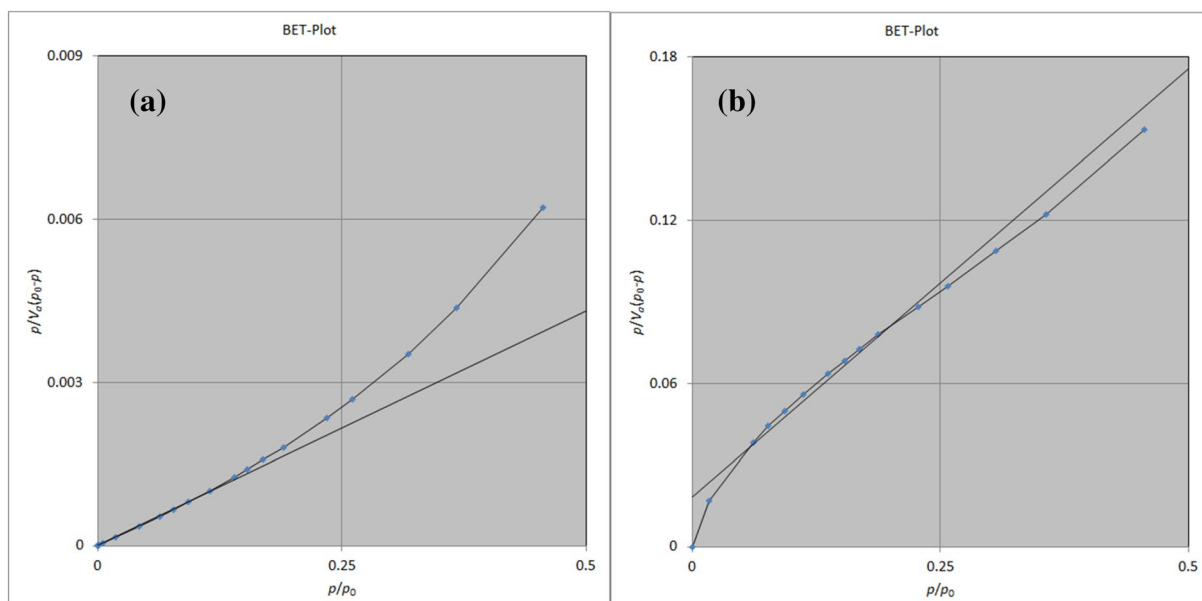
Also, BET analysis was applied to investigate the adsorption/desorption of ZIF-8/GO/MgFe$_2$O$_4$ before and after loading with by TC. As displayed in Fig. 8, the adsorption–desorption isotherm of ZIF-8/GO/MgFe$_2$O$_4$ is
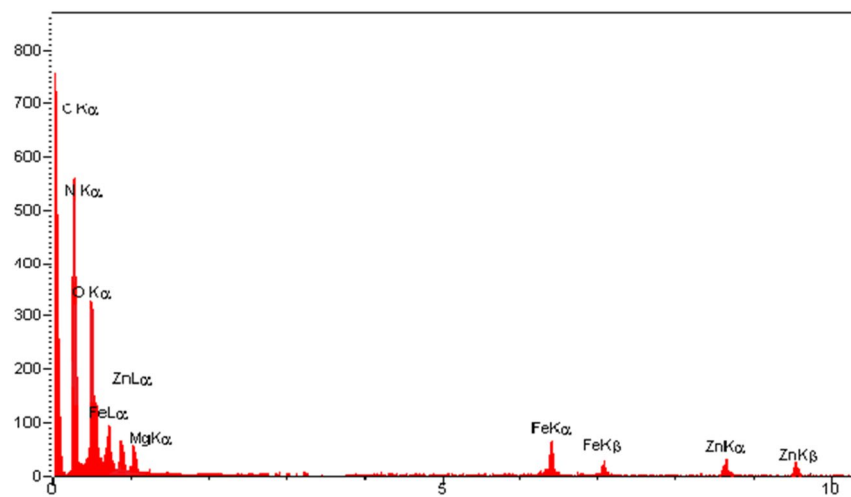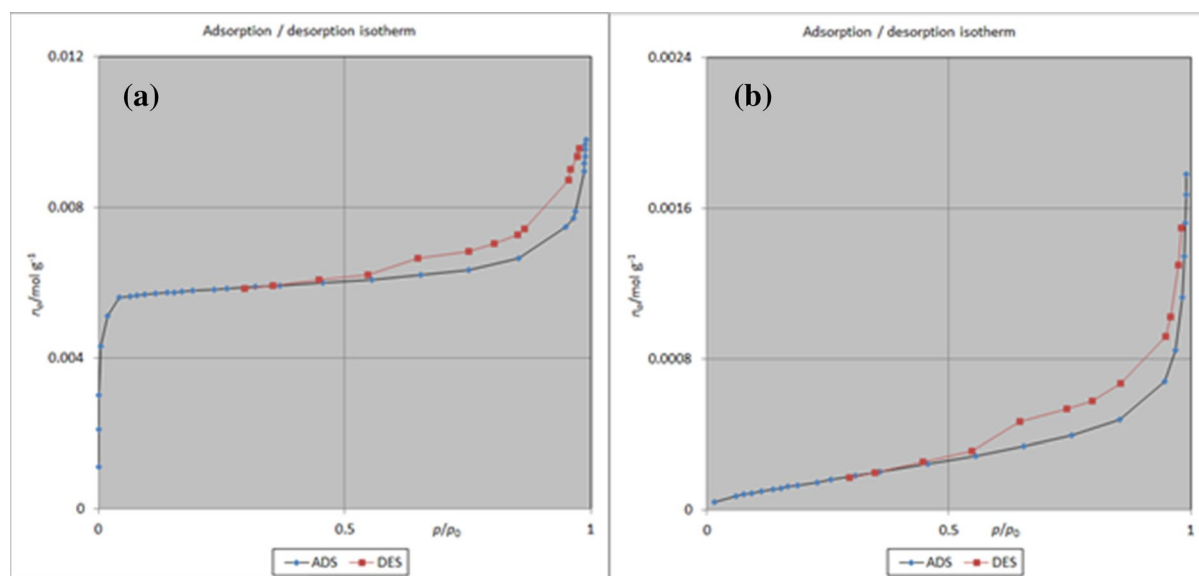
Figure 5. EDX spectrum of ZIF-8/GO/MgFe$_2$O$_4$/TC.
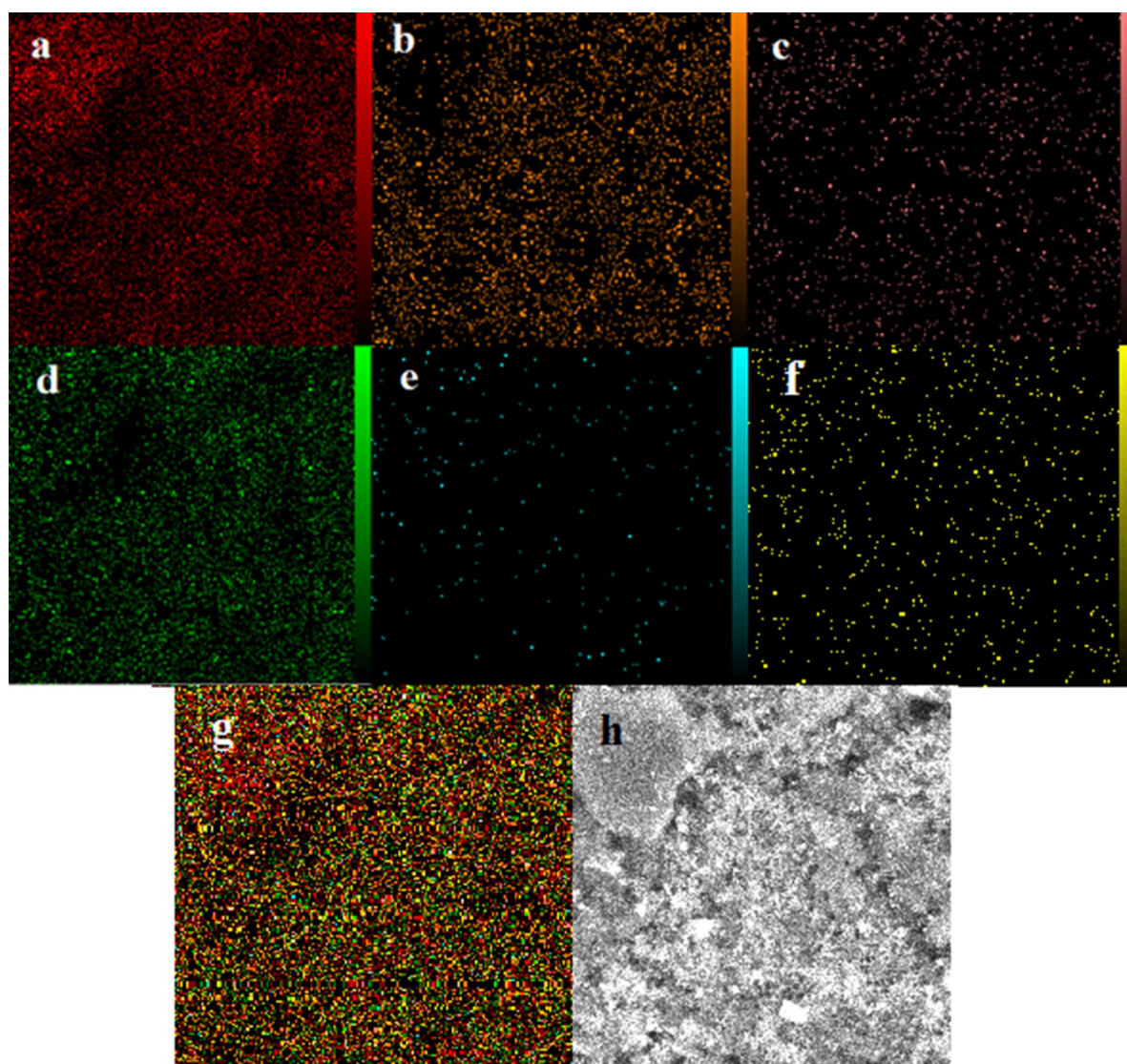
Figure 6. EDX-Mapping of the C (**a**), Fe (**b**), N (**c**), O (**d**), Zn (**e**), Mg (**f**), ZIF-8/GO/MgFe$_2$O$_4$/TC (**g**), SEM images in 10 μm (**h**).
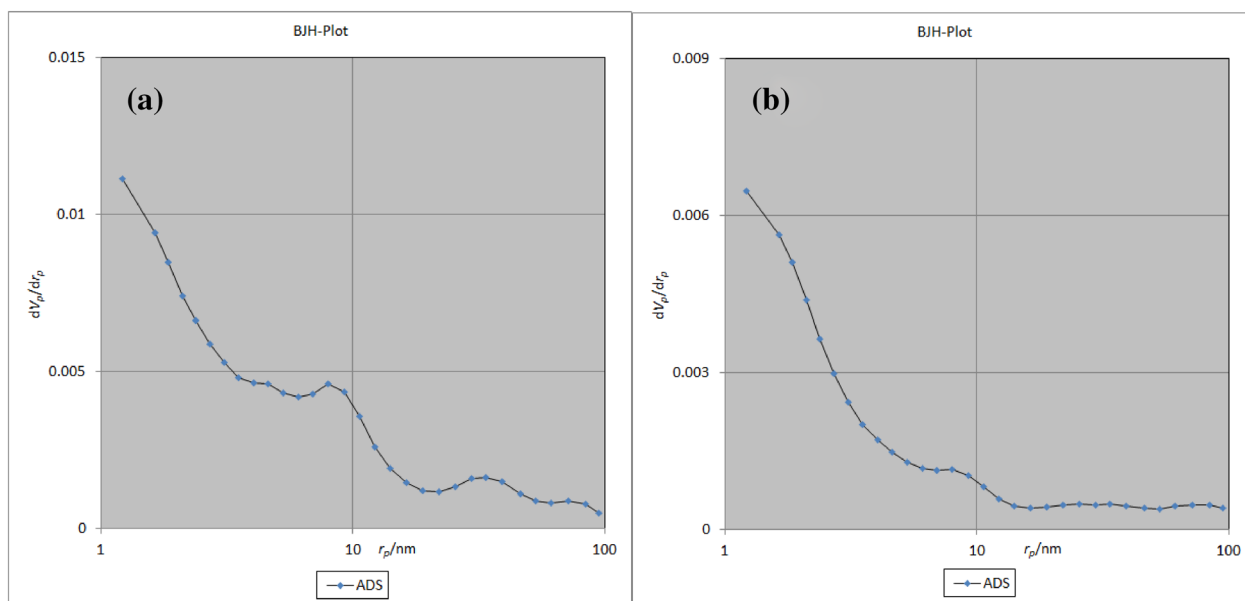
Figure 7. BET-plot of ZIF-8/GO/MgFe$_2$O$_4$ (**a**), and ZIF-8/GO/MgFe$_2$O$_4$/TC (**b**).

Figure 8. Adsorption / desorption of ZIF-8/ GO/MgFe$_2$O$_4$ (**a**), and ZIF-8/GO/MgFe$_2$O$_4$/TC (**b**).

type I[28]. The results of the BJH technique indicate that the average pore diameter are 1.21 nm, before and after drug loading (Fig. 9).

X-ray diffraction analysis. XRD technique was used to verify the structure of the prepared nanoparticles. Figure 10a shows XRD pattern of the MgFe$_2$O$_4$ nanoparticles which includes diffraction peaks at 30.1°, 35.2°, 43.1°, 57.0°, and 62.6° (2θ°) verifying the successful preparation of crystalline phase in the MgFe$_2$O$_4$[29]. In XRD pattern of ZIF-8 the peaks at 7.5°, 12.5°, and 18° (2θ°) show the formation ZIF-8 metal–organic frameworks (Fig. 10b). The XRD analysis associated with ZIF-8/MgFe$_2$O$_4$ showed that both of the synthesized materials were crystalline and their shapes is consistently based on single crystal techniques (Fig. 10c). The study of the XRD pattern of the ZIF-8/GO/MgFe$_2$O$_4$ (Fig. 10d), revealed that the presented peaks at 9.3° and 11.3° (2θ°) indicated the satisfactory cordination of the GO in the ZIF-8/MgFe$_2$O$_4$ composite. The XRD pattern of the final structure including ZIF-8/MgFe$_2$O$_4$/GO/TC (Fig. 10e), conforms the peaks at 30.1°, 35.2°, 43.1°, 57.0°, and 62.6° (2θ°) indicate the formation of the MgFe$_2$O$_4$ NPs. Also, the presence peaks at 7.5°, 12.5°, and 18° (2θ°) show the formation of the ZIF-8 frameworks, as well as, the peaks at 9.3° and 11.3° (2θ°) indicate the construction of the GO[30]. From this information it can be concluded that after loading by TC, the crystallite structure of ZIF-8/MgFe$_2$O$_4$/GO is preserved.
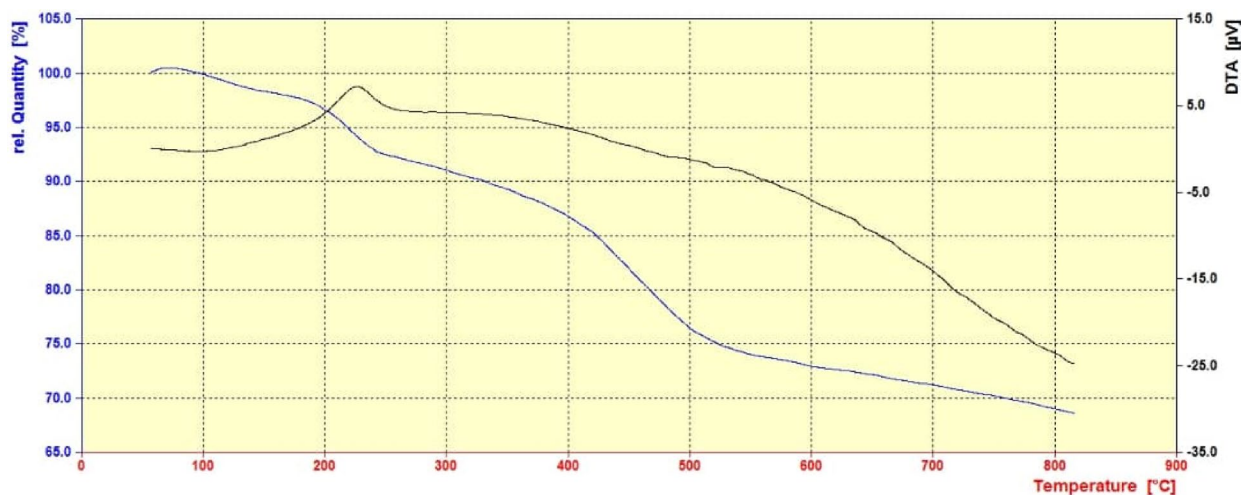
Figure 9. BJH-plot of ZIF-8/GO/MgFe$_2$O$_4$ **(a)**, and ZIF-8/GO/MgFe$_2$O$_4$/TC **(b)**.
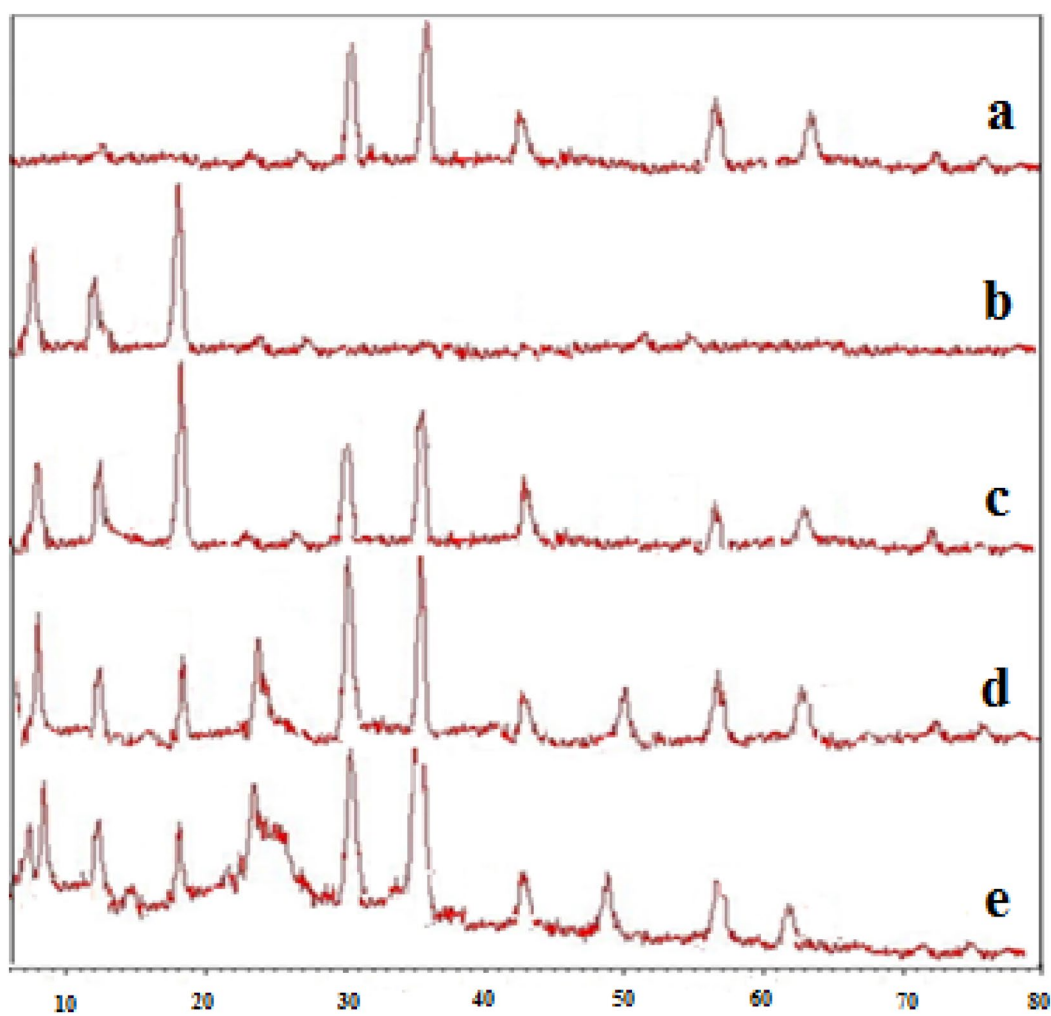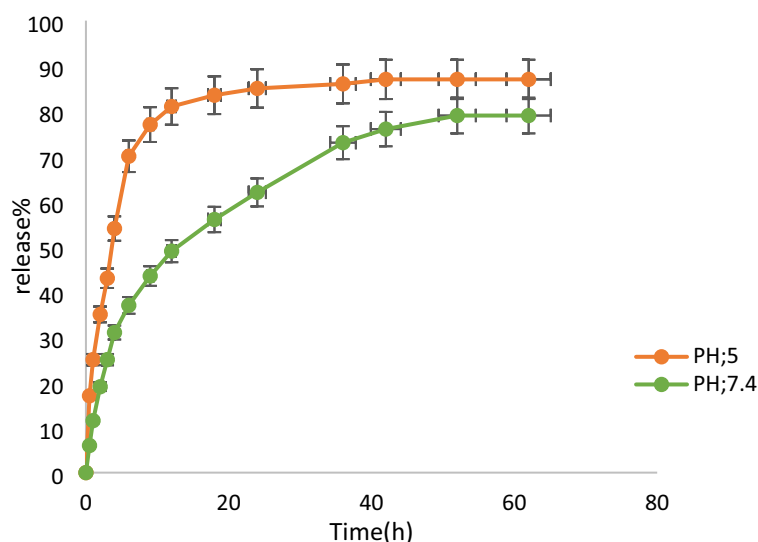

Figure 10. XRD patterns of MgFe$_2$O$_4$ **(a)**, ZIF-8 **(b)**, ZIF-8/MgFe$_2$O$_4$ **(c)**, ZIF-8/GO/MgFe$_2$O$_4$ **(d)**, and ZIF-8/MgFe$_2$O$_4$/GO/TC **(e)**.

**Figure 11.** TGA analysis of the ZIF-8/GO/MgFe$_2$O$_4$/TC.

Figure 12. TC release from ZIF-8/GO/MgFe$_2$O$_4$ in acetate buffer and phosphate buffer saline.

Thermalgravimetric analysis. TGA analysis of ZIF-8/GO/MgFe$_2$O$_4$/TC shows around 7% weight loss related to the vaporization of solvents in the 0–220 °C (Fig. 11). The weight loss about 8%, beginning from 220 to 400 °C is recognized to the devastation of TC. Moreover, the breakdown of the MOF was detected at the range of 400–500 °C. Eventually, destruction up to 800 °C is attributed to the GO[31].

Study on tetracycline release. To calculate the amount of TC loading on the nanocarrier, various concentrations of the TC were made in two buffers (pH: 5 and pH: 7.4) solutions and the absorptions were got by a UV–Vis device at a wavelength of 360 nm. Next, their calibration curves were plotted. The release diagrams at pH: 5 and pH: 7.4 are shown in Fig. 12. As displayed, the stability of ZIF-8/GO/MgFe$_2$O$_4$/TC nanocarrier at pH: 5, which was quickly destroyed in comparison with pH: 7.4, probably due to the destruction of the structure the TC release at pH: 5 was very quicker than pH: 7.4.

The achieved consequences from Fig. 12 display that the percentage of the TC release at pH: 5 increased to 80% in the first 6 h. Although, the release of the TC at physiological of the body (pH: 7.4) was near 76% over 40 h.

The results of the antimicrobial tests. Antimicrobial activities of the tetracycline and the prepared structures were performed on standard strains such as of *S. aureus* and *E. coli*. As indicated in Fig. 13 and Table 1, among various structures such as pure tetracycline, ZIF-8/GO/MgFe$_2$O$_4$, and ZIF-8/GO/MgFe$_2$O$_4$/TC, the superlative outcomes were got in the presence of ZIF-8/GO/MgFe$_2$O$_4$/TC as a strong antibacterial agent. In this research, the diameter of the zone of inhibition was evaluated after incubation to conclude the antimicrobial activity. The results revealed that TC loaded on the MOF was as well as inhibited the development of both
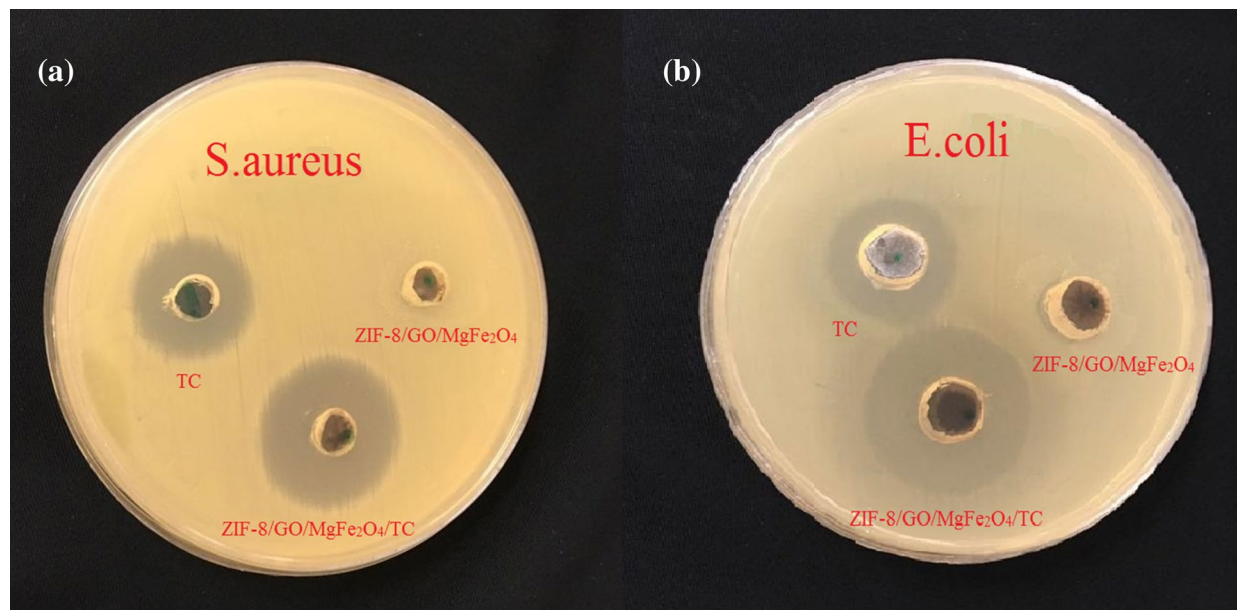
Figure 13. Results of antibacterial tests **(a)** plate containing *Staphylococcus aureus*, and **(b)** plate containing *Escherichia coli* bacteria.

Bacterium	TC	ZIF-8/GO/MgFe₂O₄	ZIF-8/GO/MgFe₂O₄/TC
E.coli	17 mm	0	22 mm
S.aureus	18 mm	0	25 mm

Table 1. The antibacterial activity of TC, ZIF-8/GO/MgFe₂O₄, ZIF-8/GO/MgFe₂O₄/TC.

bacteria. Therefore, it can be established that the use of ZIF-8/GO/MgFe$_2$O$_4$ as nanocarrier can increase the antibacterial activities of the TC.

As shown in Table 1, inhibition zone of 22 mm against *E. coli* and 25 mm related to *S. aureus*, such results are obtained when the tetracycline of an inhibitory behavior is shown against *S. aureus* and *E. coli*. With an inhibition zone of 17 mm and 18 mm, respectively.

Conclusion

The outcomes of this study revealed that the novel nanostructure including ZIF-8/GO/MgFe$_2$O$_4$ was successfully synthesized based on the characterization and structure elucidation by SEM, EDX/Mapping, XRD, BET, FT-IR, and TGA analysis. In addition, the tetracycline as an antibiotic drug was encapsulated into the ZIF-8/GO/MgFe$_2$O$_4$ with high loading of 90%, due to the porous nanocomposite, great surface area and cavities in the structure of nanocarrier. In addition, the TC release from the nanocomposite were 88% and 92%, phosphate buffer saline and acetate buffer, respectively. In order to evaluate the antibacterial activities of the prepared composites toward pure tetracycline, the results of by agar well diffusion showed that the antibacterial activity of ZIF-8/GO/MgFe$_2$O$_4$/TC is more than ZIF-8/GO/MgFe$_2$O$_4$ and TC.

References

1. Fang, X. *et al.* Nanocomposites of Zr(IV)-based metal-organic frameworks and reduced graphene oxide for electrochemically sensing ciprofloxacin in water. *ACS Appl. Nano Mater.* **2**, 2367–2376 (2019).
2. Daghrir, R. & Drogui, P. Tetracycline antibiotics in the environment: A review. *Environ. Chem. Lett.* **11**, 209–227 (2013).
3. Chopral, I. & Roberts, M. Tetracycline antibiotics: Mode of action, applications, molecular biology, and epidemiology of bacterial resistance. *Microbiol. Mol. Biol. Rev.* **65**, 232–260 (2001).
4. Zhu, Y. *et al.* Graphene and graphene oxide: Synthesis, properties, and applications. *Adv. Mater.* **22**, 3906–3924 (2010).
5. Karimzade, Z., Javanbakht, S. & Namazi, H. Carboxymethylcellulose/MOF-5/graphene oxide bio-nanocomposite as antibacterial drug nanocarrier agent. *BioImpacts.* **9**, 5–13 (2019).
6. Mohammadi, O., Golestanzadeh, M. & Abdouss, M. Recent advances in organic reactions catalyzed by graphene oxide and sulfonated graphene as heterogeneous nanocatalysts: A review. *New J. Chem.* **41**, 11471–11497 (2017).
7. Cao, K. *et al.* Fabrication of BTA-MOF-TEOS-GO nanocomposite to endow coating systems with active inhibition and durable anticorrosion performances. *Prog. Org. Coat.* **143**, 1–14 (2020).
8. Huxford, R. C., Della Rocca, J. & Lin, W. Metal–organic frameworks as potential drug carriers. *Curr. Opin. Chem. Biol.* **14**, 262–268 (2010).

9. Sun, K. *et al*. Functionalization of mixed ligand metal-organic frameworks as the transport vehicles for drugs. *J. Colloid Interface Sci*. **486**, 128–135 (2017).
10. Sun, Ch., Qin, Y., Wang, X. L. & Su, Z. M. Metal-organic frameworks as potential drug delivery systems. *Expert Opin. Drug Deliv*. **10**, 89–101 (2013).
11. Uyen, P. N., Tran, K. Y. K., Led, A., Nam, T. & Phan, S. Expanding applications of metal–organic frameworks: Zeolite imidazolate framework ZIF-8 as an efficient heterogeneous catalyst for the Knoevenagel reaction. *ACS Catal*. **1**, 120–127 (2011).
12. Esfahanian, M., Ghasemzadeh, M. A. & Razavian, S. M. H. Synthesis, identification and application of the novel metal-organic framework Fe$_3$O=@PAA@ZIF-8 for the drug delivery of ciprofloxacin and investigation of antibacterial activity. *Artif. Cell Nanomed. Biotech*. **47**, 2024–2030 (2019).
13. Rostami, M., Aghajanzadeh, M., Zamani, M., Kheiri Manjili, H. & Danafar, H. Sono-chemical synthesis and characterization of Fe$_3$O$_4$@mTiO$_2$-GO nanocarriers for dual-targeted colon drug delivery. *Res. Chem. Intermed*. **44**, 1889–1904 (2018).
14. Mody, V. V. *et al*. Magnetic nanoparticle drug delivery systems for targeting tumor. *Appl. Nanosci*. **4**, 385–392 (2014).
15. Nasrabadi, M., Ghasemzadeh, M. A. & Zand Monfared, M. R. Preparation and characterization of UiO-66 metal-organic frameworks for the drug delivery of ciprofloxacin and evaluation of their antibacterial activities. *New J. Chem*. **43**, 1–15 (2019).
16. Dong, H. *et al*. Folic acid-functionalized Zr-based metal-organic frameworks as drug carriers for active tumor-targeted. *Chem. Eur. J*. **24**, 17148–17154 (2018).
17. Gua, W. *et al*. L-cysteine decorated nanoscale metal-organic frameworks delivery valprroic acid/cisplatin for drug-resistant lung cancer therapy. *Chem. Commun*. **56**, 3919–1922 (2020).
18. Wu, M. X. & Yang, Y. W. Metal-organic framework (MOF)-based drug/cargo delivery and cancer therapy. *Adv. Mater*. **29**, 1–20 (2017).
19. Javanbakht, S., Nezhad Mokhtari, P., Shaabani, A., Arsalani, N. & Ghorbani, M. Incorporating Cu-based metal-organic framework/drug nanohybrids into gelatin microsphere for ibuprofen oral delivery. *Mater. Sci. Eng*. **96**, 302–309 (2019).
20. Sun, Y. *et al*. Nanocarriers for drug delivery in biomedical applications. *Nanomicro. Lett*. **12**, 1–29 (2020).
21. Zheng, H. *et al*. One-pot synthesis of metal-organic frameworks with encapsulated target molecules and their applications for controlled drug delivery. *J. Am. Chem. Soc*. **138**, 962–968 (2016).
22. Gao, X., Hai, X., Baigude, H., Guan, W. & Liu, Zh. Fabrication of functional hollow microspheres constructed from MOF shells: Promising drug delivery systems with high loading capacity and targeted transport. *Sci. Rep*. **6**, 1–10 (2016).
23. Liu, Y., Zhang, P., Fan, M. & Jiang, P. Biodiesel production from soybean oil catalyzed by magnetic nanoparticle MgFe$_2$O$_4$@CaO. *Fuel* **164**, 314–321 (2016).
24. Adhikari, C., Das, A. & Chakraborty, A. Zeolitic imidazole iramework (ZIF) nanospheres for easy encapsulation and controlled release of an anticancer drug doxorubicin under different external stimuli: A way toward smart drug delivery system. *Mol. Pharm*. **12**, 3158–3166 (2017).
25. Naeimi, H. & Golestanzadeh, M. Highly sulfonated graphene and graphene oxide nanosheets as heterogeneous nanocatalysts in green synthesis of bisphenolic antioxidants under solvent free conditions. *RSC Adv*. **4**, 56475–56488 (2014).
26. Akbari, M., Ghasemzadeh, M. A. & Fadaeian, M. Synthesis and application of ZIF-8 MOF incorporated in a TiO$_2$@chitosan nanocomposite as a strong nanocarrier for the drug delivery of acyclovir. *ChemistrySelect* **5**, 14564–14571 (2020).
27. Kang, J., Liu, H., Zheng, Y. M., Qu, J. & Chen, J. P. Systematic study of synergistic and antagonistic effects on adsorption of tetracycline and copper onto a chitosan. *J. Colloid Interface Sci*. **344**, 117–125 (2010).
28. Zhang, O., Jia, Y. & Hou, L. Synthesis of zeolitic imidazolate framework-8 on polyester fiber for PM$_{2.5}$ removal. *RSC Adv*. **8**, 31471–31477 (2018).
29. Verma, S., Joy, P. A., Khollam, Y. B., Potdar, H. S. & Deshpande, S. B. Synthesis of nanosized MgFe2O4 powders by microwave hydrothermal method. *Mater. Lett*. **58**, 1092–1095 (2004).
30. Mozafari, R., Ghadermazi, M. & Nickel, A. Nanoparticle engineered CoFe2O4@GO-Kryptofix 22 composite: A green and retrievable catalytic system for the synthesis of 1,4-benzodiazepines in water. *RSC Adv*. **10**, 15042–15064 (2020).
31. Uregen, N., Pehlivanoğlu, K., Ozdemir, Y. & Devrim, Y. Development of polybenzimidazole/graphene oxide composite membranes for high temperature PEM fuel cells. *Int. J. Hydrog. Energy*. **42**, 2636–2647 (2018).

Acknowledgements

Author contributions

S.S.-R. and M.A.G. wrote the main manuscript and S.S.-R. and S.M.H.R. prepared figures. All authors reviewed the manuscript.

Competing interests

The authors declare no competing interests.

Additional information

Correspondence and requests for materials should be addressed to M.A.G.

Reprints and permissions information is available at www.nature.com/reprints.

Publisher's note Springer Nature remains neutral with regard to jurisdictional claims in published maps and institutional affiliations.